

# Orbital magnetism and magnetic anisotropy in thin-film ferromagnets disturbed from the ground state

L. M. Sandratskii

*Max-Planck-Institut für Mikrostrukturphysik, Weinberg 2, 06120 Halle, Germany*

(Received 21 March 2013; revised manuscript received 14 July 2013; published 19 August 2013)

We report first-principles study of the orbital magnetism and magnetic anisotropy energy (MAE) in ultrathin films of Fe, Co, and FePt disturbed from the ferromagnetic ground state. The deviation of ferromagnetic spin configurations from the easy axis leads to the noncollinearity of the spin and orbital moments. In Fe and Co, this noncollinearity correlates with the magnitude of MAE. In contrast, in FePt a complex interplay of competing processes leads to unusual phenomenon of the orthogonality of the inducing spin and induced orbital moments. Considering the influence of noncollinearity of spin moments we obtain opposite trends in the MAE variation for Fe and Co films. This finding correlates with the absence of universal temperature behavior of MAE in itinerant magnets and is shown to originate in the variation of the electronic structure with the change of spin configuration.

DOI: [10.1103/PhysRevB.88.064415](https://doi.org/10.1103/PhysRevB.88.064415)

PACS number(s): 75.30.Gw, 75.70.Ak, 75.70.Tj

## I. INTRODUCTION

The orbital magnetism is a fundamental property of magnetic materials. Being closely connected to the spin-orbit coupling (SOC) it provides the tool for deeper understanding of this important interaction giving the origin to numerous physical effects.<sup>1–4</sup> An enormous success in the fabrication of new nanoscale materials with enhanced orbital magnetism increased further the importance of this phenomenon.

On the experimental side an important progress in the study of orbital magnetism was achieved with the development of the methods of x-ray magnetic circular dichroism spectroscopy (XMCDs) that allow separate determination of spin and orbital atomic moments.<sup>5</sup> Recently, Boeglin *et al.* reported the observation of *distinct dynamics* of two types of magnetic moments.<sup>6</sup> One can expect important connections between the properties of the materials excited by laser light<sup>6</sup> and these materials at nonzero temperatures since in both cases the absorption of energy disturbs the magnetic system from the ground state. The experimental data collected for itinerant-electron magnets show that the simple picture of the temperature dependence of magnetic anisotropy developed for localized-moment systems<sup>7</sup> fails for these materials and the derivation of a unified law seems unfeasible.<sup>8–10</sup> On the other hand, for the ground magnetic state of itinerant ferromagnets there is the widely accepted concept of Bruno<sup>11</sup> stating the proportionality  $\text{MAE} = -\frac{\xi}{4\mu_B} \Delta m_o$  of the magnetic-anisotropy energy (MAE) to the anisotropy of the orbital moment  $\Delta m_o$ . Here MAE and  $\Delta m_o$  are the differences of the energy and orbital moment for the states of the system with spin magnetization parallel to the easy and hard magnetization axes;  $\xi$  is the effective parameter of the SOC.

The purpose of this paper is to make a step in the understanding of the orbital magnetism of metallic systems disturbed from the magnetic ground state. We consider three free-standing 1 ML thick films of Fe, Co, and FePt. Our aim here is not the detailed description of a concrete experiment on a particular system. Instead, we aim to demonstrate the variety of behavior and to discuss its origin. Because of strong structural anisotropy of thin films the effects we

study are enhanced, which makes thin films an ideal model object.

We report first-principles calculations for two types of spin states. First, keeping the spin structure collinear we rotate it between the easy and hard axes studying the characteristics of the system as the function of the rotation angle  $\theta_s$ . In the absence of the SOC all physical quantities are invariant with respect to the rotation and the orbital moment is zero. The SOC leads to unquenching of the orbital moment and makes physical quantities  $\theta_s$  dependent. It is known that the orbital moment induced by the SOC is in general noncollinear to the inducing spin moment.<sup>12–14</sup> We will show that for the Fe and Co films the results of first-principles calculations fit well in the expected picture suggesting the existence of a simple relation between the noncollinearity of the two moments and the strength of the MAE.<sup>13</sup> On the other hand, in the case of FePt our study reveals a surprising phenomenon of the orthogonality of the inducing spin and induced orbital moments. This orthogonality is an important feature of the system reflecting the presence of competing processes in the formation of the physical characteristics governed by SOC.

On the next step, we consider noncollinear spin configurations. By taking different angles between atomic spins we simulate the extent of the spin disorder. Similar to the calculation for collinear spin structures we rotate noncollinear spin configurations with respect to the crystallographic axes calculating the dependence of the physical quantities on both the angle between atomic spins and the direction of the net spin moment. As mentioned above, the remarkable feature of the experimental situation for itinerant magnets is the absence of a universal temperature behavior of the MAE: the MAE can both decrease and increase with increasing temperature and the microscopic understanding of this diversity remains a challenge. We will show that, in correlation with experiment, the Fe and Co films demonstrate opposite types of the dependence on increasing spin noncollinearity: in Co, the MAE decreases with increasing spin noncollinearity, whereas in Fe a strong increase of the MAE is obtained. We explain the difference of the behavior by the dependence of the electronic structure on spin noncollinearity.

## II. CALCULATION TECHNIQUE

The calculations are performed with the ASW method generalized to account for SOC and noncollinear magnetism.<sup>12</sup> The latter includes both the noncollinearity of the spin moments and the noncollinearity between spin and orbital moments. Under such conditions the electron states lose spin projection as a good quantum number and must be treated as two-component spinors. Respectively, the electron potential takes the form of the 2 by 2 matrix.

Assuming a spherically symmetric form of the atomic potentials the effective potential in  $i$ th atomic sphere can be written in the form

$$V_i(r) = U(\theta_i, \phi_i)^\dagger \begin{pmatrix} V_i^+(r) & 0 \\ 0 & V_i^-(r) \end{pmatrix} U(\theta_i, \phi_i), \quad (1)$$

where angles  $\theta_i$  and  $\phi_i$  determine the local spin-coordinate system of the  $i$ th atom characterized by the diagonal form of the potential matrix;  $V_i^+$  and  $V_i^-$  are the spin-up and spin-down potentials in the local system;  $U(\theta_i, \phi_i)$  is the matrix of spin- $\frac{1}{2}$  rotation transforming the potential from the atomic system of the  $i$ th atom to the global system.

The noncollinear spin structures are characterized by different values of angles  $\theta_i$  and  $\phi_i$  for different atoms. The operator of the spin-orbit coupling is taken in the form

$$\mathbf{H}_{so} = \frac{1}{(2c)^2} \frac{1}{r} \left[ \begin{pmatrix} \frac{1}{M_+^2} \frac{dV_+}{dr} & 0 \\ 0 & \frac{1}{M_-^2} \frac{dV_-}{dr} \end{pmatrix} \sigma_z \hat{L}_z + \frac{1}{M_{av}^2} \frac{dV_{av}}{dr} (\sigma_x \hat{L}_x + \sigma_y \hat{L}_y) \right], \quad (2)$$

where

$$V_{av}(r) = \frac{1}{2} (V_+(r) + V_-(r)) \quad (3)$$

and

$$M_\alpha = \frac{1}{2} \left( 1 - \frac{1}{c^2} V_\alpha \right), \quad \alpha = av, +, -. \quad (4)$$

$\sigma_x, \sigma_y, \sigma_z$  are the Pauli matrices and  $\hat{L}_x, \hat{L}_y, \hat{L}_z$  are the operators of the components of the orbital momentum. In Eqs. (2) and (4), the Rydberg atomic units are used.

Not only the spin moment but also the orbital moment is treated as a three-dimensional vector. The  $\alpha$  projection of the orbital momentum of the  $i$ th atom is obtained as the sum of expectation values of the angular momentum operator  $\hat{L}_\alpha$  for occupied electron states:

$$m_{o\alpha}^i(E) = \sum_{\mathbf{k}n, \epsilon_{\mathbf{k}}^n < E} \int_{\Omega_i} \psi_{\mathbf{k}}^{n+}(\mathbf{r}) \hat{L}_\alpha \psi_{\mathbf{k}}^n(\mathbf{r}) d\mathbf{r}, \quad \alpha = x, y, z, \quad (5)$$

where  $n$  is the band index and the integration is carried out over the  $i$ th atomic sphere,  $\psi_{\mathbf{k}}^n$  are spinor wave functions, and  $\epsilon_{\mathbf{k}}^n$  energies of the electron states. Energy parameter  $E$  governs the filling of the electronic bands. Actual value of the momentum corresponds to  $E$  equal to the Fermi energy.

In the cases of Fe and Co the calculations were performed for 1 ML square lattices. For the FePt two atomic layers of the  $L1_0$  structure were considered.

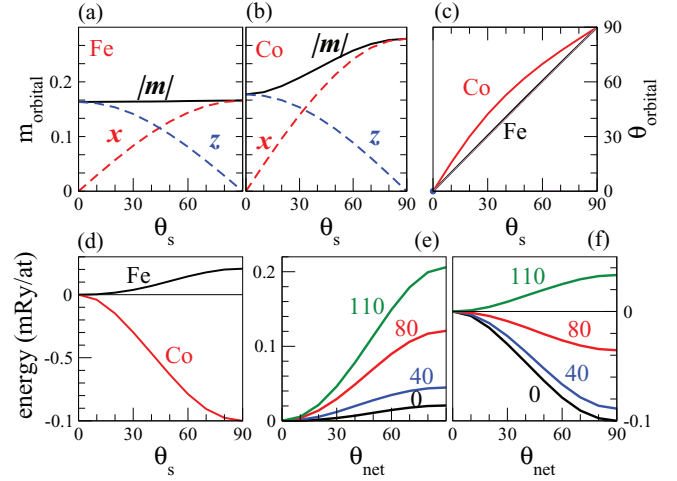


FIG. 1. (Color online) Calculated properties for Fe and Co films. (a) Module and  $x$  and  $z$  projections of the orbital moment of Fe film for ferromagnetic spin configurations as a function of  $\theta_s$ ; (b) the same as (a) but for Co film; (c) direction of the orbital moment as a function of the direction of the spin moment for ferromagnetic spin configuration of both Fe and Co; (d) the energy of the Fe and Co films for ferromagnetic configurations as a function of  $\theta_s$ ; (e) the energies of noncollinear spin configurations of Fe as a function of the direction of the net spin magnetization; the numbers at the curves give the angles between local atomic spin axes. (f) Same as (e) but for Co film.

## III. RESULTS AND DISCUSSION

### A. Ferromagnetic spin configurations

In Fig. 1 we present calculational results for ferromagnetic structures of the Fe and Co films with spin moments assuming different directions within  $xz$  plane. (The  $z$  axis is orthogonal to the film.) The  $\theta_s$  dependence of the  $m_{ox}$  and  $m_{oz}$  is well described as  $m_{ox} = M_{ox} \sin \theta_s$  and  $m_{oz} = M_{oz} \cos \theta_s$ . Because of different amplitudes  $M_{ox}$  and  $M_{oz}$  of two components the spin and orbital moments are noncollinear. The maximal angle between spin and orbital moments is given by  $\cos \theta_{o-s} = 2\sqrt{M_{ox}M_{oz}}/(M_{ox} + M_{oz})$ .

For Fe, the amplitudes  $M_{ox}$  and  $M_{oz}$  are very close to each other [Fig. 1(a)]. As a result the noncollinearity of the spin and orbital moments is small [Fig. 1(c)]. The MAE is also weak [Fig. 1(d)]. On the opposite, in the Co film the difference of the amplitudes of two components is large [Fig. 1(b)] leading to the angle between spin and orbital moments of  $13^\circ$  for  $\theta_s \approx 38^\circ$ . The Co MAE is also strongly increased and has the expected sign [Fig. 1(d)]: the easy axis corresponds to a larger orbital moment.

The origin of the difference between Fe and Co films is in the properties of the electronic structures of the two films. We illustrate this by comparing the components of the orbital moments calculated as a function of band occupation [Eq. (5)]. All dependences presented in Fig. 2 have the same characteristic shape consisting of one negative peak at lower energies and one positive peak at higher energies. This common shape can be explained as follows. The occupation of the  $3d$  states of the ferromagnetic systems begins with the spin-up states lying, because of the exchange splitting, at lower energies than the spin-down states. The  $\hat{L}_z \sigma_z$  part of the SOC

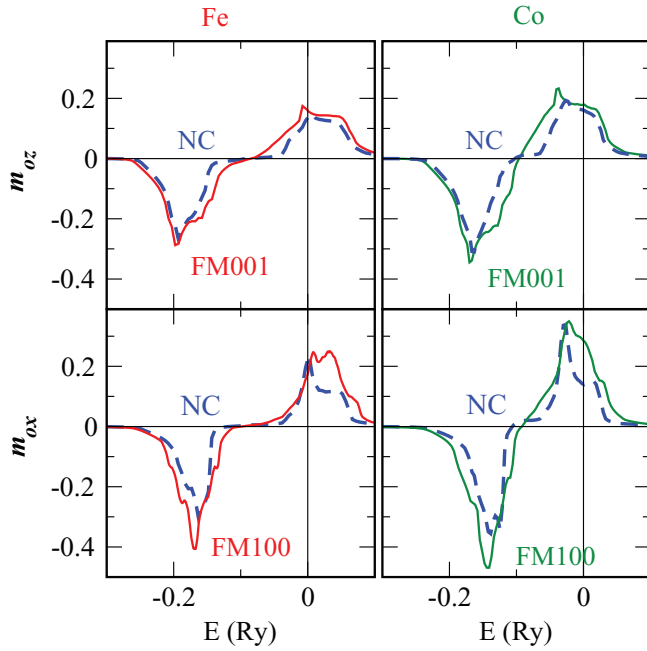


FIG. 2. (Color online)  $z$  components (upper panels) and  $x$  components (lower panels) of the atomic orbital moments of Fe film (left panels) and Co film (right panels) as a function of the band occupation. Three magnetic configurations are considered: ferromagnetic moments collinear to  $z$  axis (FM001), ferromagnetic moments collinear to  $x$  axis (FM100), and noncollinear configuration (NC, broken curves) with local atomic spin axes<sup>12</sup> deviating by  $40^\circ$  in opposite directions from the  $z$  axis. The energy origin is at the Fermi level.

[Eq. (2)] shifts the orbitals with negative quantum number  $m$  to lower energies and orbitals with positive  $m$  to higher energies. Correspondingly, the orbital moment first becomes antiparallel to the spin moment until the filling of the positive- $m$  orbitals compensates the disbalance between the occupation of the  $+m$  and  $-m$  orbitals. The second higher-energy peak corresponds to the spin-down orbitals. Here the trend in the  $\pm m$  polarization due to the SOC is opposite leading to the formation of the positively directed orbital moment. Since the spin-down states in Fe and Co are not completely filled the compensation of the  $m$  and  $-m$  orbitals does not take place resulting in an orbital moment with positive projection on the direction of the spin moment.

The details of the modification of the electronic structure by the SOC depend on the direction of the spin moments with respect to the crystallographic axes. For both Fe and Co the  $m_{ox}(E)$  and  $m_{oz}(E)$  curves are rather different. However, at the Fermi level,  $E_F$ , the values of  $m_{ox}$  and  $m_{oz}$  of Fe are very close to each other, whereas for Co,  $m_{ox}(E_F)$  is distinctly larger than  $m_{oz}(E_F)$ . The sensitivity to the details of the electron structure including the different level of the occupation explains why, despite similar strength of the SOC, the calculated MAE and anisotropy of the orbital moment are different for Fe and Co.

In FePt the character of the  $\theta_s$  dependence of the SOC-induced quantities is complex and unexpected (Fig. 3). First, despite parallel spin moments of the Fe and Pt atoms their orbital moments behave very differently. The both orbital moments are parallel to each other and to the spin moments

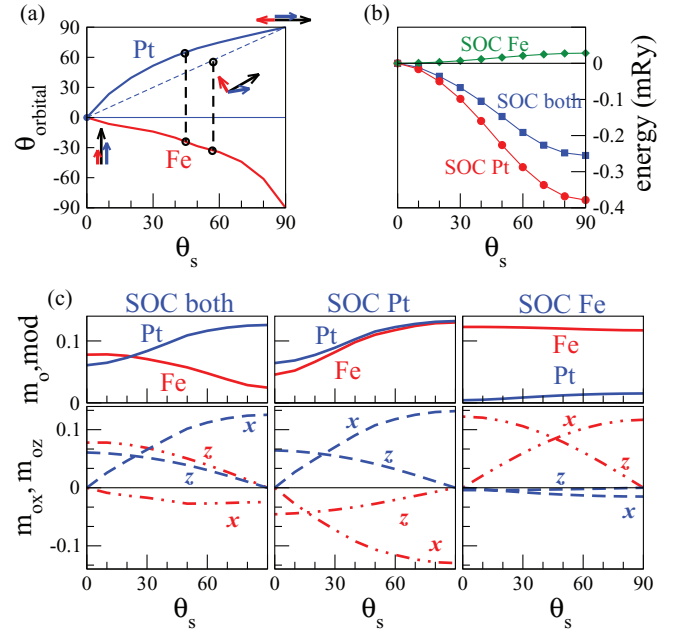


FIG. 3. (Color online) Results of calculations for FePt film. (a) The directions of the Fe and Pt orbital moments as a function of the direction of the ferromagnetic spin moments. The sloping broken line corresponds to  $\theta_o = \theta_s$ . Vertical lines connect the points corresponding to orthogonal vectors. Three arrow inserts show relative directions of the spin and orbital moments at the ends and inside the  $\theta_s$  interval. (b) Energy as a function of  $\theta_s$  for SOC on both atoms or only on one of them. (c) The lower panels show the magnitude and projections of the orbital moments for SOC on both atoms or only on one of them. Dashed lines give the Pt projections and dashed-dotted lines the Fe projections.

only for  $\theta_s = 0$ . With spin moments of all atoms moving from the  $z$  axis towards the  $x$  axis the orbital moments of the Fe and Pt atoms deviate in opposite directions from the  $z$  axis. At  $\theta_s \approx 57^\circ$  the spin and orbital atomic moments of Fe atoms become orthogonal to each other. At  $\theta_s \approx 45^\circ$  the orbital moments of Fe and Pt are orthogonal.

To understand this complex behavior we performed calculations with the SOC switched off on one of the atomic types [Fig. 3(c)]. For the SOC on the Pt atoms only we obtain large induced Fe orbital moment whose magnitude follows closely the magnitude of the Pt orbital moment. The angle between two orbital moments is  $180^\circ$  for  $\theta_s = 0$  and  $\theta_s = 90^\circ$  and close to this value for intermediate  $\theta_s$ . For the SOC only on the Fe atoms the induced Pt orbital moment is small. The Fe orbital moments are exactly parallel to the spin moments for  $\theta_s = 0$  and  $\theta_s = 90^\circ$  and deviate from the spin moments very weakly for all intermediate  $\theta_s$ . The MAE increases strongly with the SOC switched on only on the Pt atoms and drops to a small value for the SOC on Fe atoms only.

These calculations for the FePt film lead to the following physical picture. The atomic orbital moments have two different contributions: one induced by the SOC on the given atom and the other induced by the hybridization with the states of other atoms  $\pm m$  polarized by the SOC on these atoms. For Fe atoms both contributions are comparable. For  $\theta_s = 90^\circ$  ( $x$  axis) the influence of the SOC on Pt is stronger than the influence of

the own SOC and the Fe orbital moment is antiparallel to the spin magnetization. On the other hand, for  $\theta_s = 0^\circ$  ( $z$  axis) the influence of the own SOC is stronger resulting in the Fe orbital moment parallel to the spin magnetization. The  $\theta_s$  variation of the energy contributions due to the own SOC follows well Bruno's model: larger orbital moment—lower energy. The energy contributions to the MAE because of the SOC on the other atom does not follow this rule.<sup>15</sup> The orthogonality of the spin and orbital Fe moments in the FePt film reflects the competition of different trends resulting from the SOC on two inequivalent types of atoms.

### B. Noncollinear spin configurations

The consideration of the collinear spin configurations is not sufficient to study the systems disturbed by laser light or heating since in both cases the atomic spins become noncollinear. If we assume that the MAE is largely determined by the single-site contribution and that the parameters of the single-site anisotropy do not change with spin disorder the prediction is feasible. Let us consider a configuration of noncollinear spins with the net moment parallel to the ferromagnetic easy axis and the same spin configuration with all moments rotated by  $90^\circ$ . If each atomic moment gives an independent contribution to the MAE determined by the monotonous function  $E_{FM}(\theta_s)$  of the types shown in Figs. 1 and 3, the MAE per atom can only decrease with disordering. The energy of the noncollinear spin configuration as a function of the direction of the net magnetization  $\theta_{\text{net}}$  should get the form of flattened  $E_{FM}(\theta_s)$  curve with flattening increasing with increasing noncollinearity.

To verify this scenario we increased the size of the unit cell to include two  $3d$  atoms. The angle between the local atomic spin axes<sup>12</sup> of these atoms was fixed to  $\theta_{\text{inter}}$  and the spin configuration was rotated within the  $xz$  plane in such a way that the direction of the net spin moment changes from the  $z$  axis ( $\theta_{\text{net}} = 0$ ) to the  $x$  axis ( $\theta_{\text{net}} = 90^\circ$ ). The flattening scenario works rather well for the Co film and  $\theta_{\text{inter}}$  up to about  $90^\circ$  [Figs. 1(f) and 4]. In Fe, instead of decrease with raising spin noncollinearity the MAE strongly increases [Figs. 1(e) and 4]. This striking difference in the behavior of two films resembles the variety of the experimental behavior of the MAE in itinerant-electron systems showing that MAE can both decrease and increase with increasing temperature.<sup>8,16</sup>

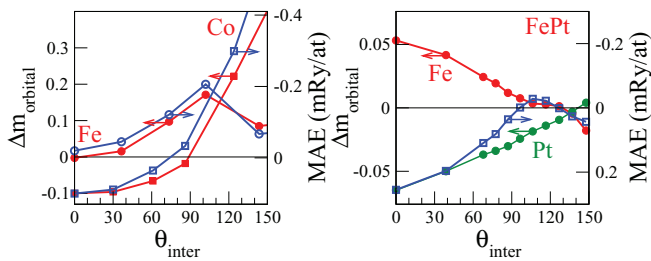


FIG. 4. (Color online) Anisotropy of the orbital moment and the MAE for noncollinear magnetic configurations with different angles between atomic spins for Fe, Co (left) and FePt (right) films. The direction of the MAE axis is reversed. The arrows show the direction to the ordinate axis corresponding to the curve.

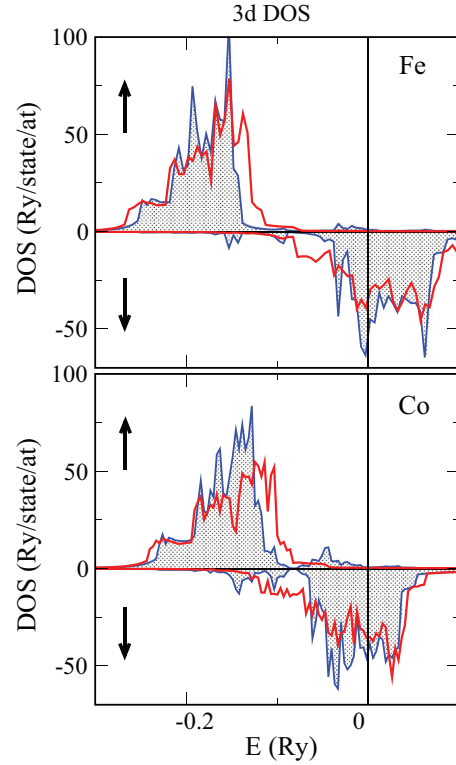


FIG. 5. (Color online) Spin-projection resolved  $3d$  DOS of Fe and Co films. The red curves give the DOS of the ferromagnetic configurations with the spins parallel to the  $z$  axis. The filled blue lines correspond to the noncollinear spin configurations with angle  $80^\circ$  between local atomic axes of the two magnetic atoms in the unit cell. The direction of the net spin moment is parallel to the  $z$  axis. For noncollinear spin configuration the spin projections are given with respect to the local atomic axes.

The explanation of the absence of a universal behavior is in the variation of the electronic structure with spin disorder that is neglected if temperature-independent anisotropy constants are assumed. The noncollinearity of spin moments leads to strong reconstruction of the electronic structure. The details of the reconstruction depend on both the concrete system and the concrete magnetic configuration. In Fig. 5 we show spin-projection resolved  $3d$ -DOS for both collinear ferromagnetic configuration and a selected configuration with noncollinear spin moments. The noncollinear configurations presented are characterized by angle  $80^\circ$  between the local spin axes of the pairs of atoms in the unit cell. For both Fe and Co there is strong reconstruction of the DOS. In the noncollinear case the peaks of the  $3d$  states become higher and narrower. In Fe, there is a particularly strong reconstruction in the energy region around the Fermi energy. The reconstruction of the electronic structure is a strong source of the system-dependent behavior with increasing noncollinearity of the atomic spin moments. Note that the narrowing in energy of some groups of the electronic states can be considered as an expected effect resulting from the hybridizational repulsion of the ferromagnetic spin-up and spin-down states caused by the noncollinearity of the atomic moments.<sup>12</sup> This finding is in interesting correlation with the experimentally detected shrinking bandwidth in ferromagnetic Ni after optical femtosecond laser excitation.<sup>17</sup>



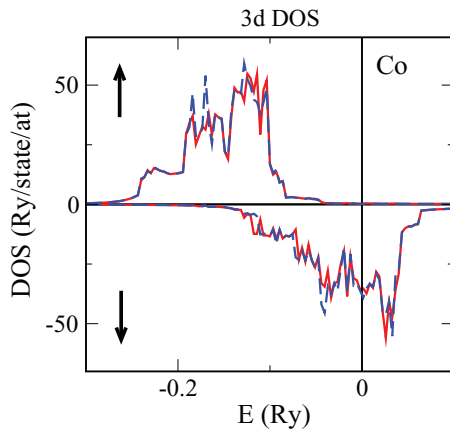


FIG. 6. (Color online) Difference between 3d DOS of Co film with (solid red curve) and without (broken blue curve) SOC.

The consequences of the SOC appear as relatively weak further modifications of the electronic structure and therefore depend on this reconstruction. This is illustrated in Fig. 6 for the collinear spin configuration of the Co film. Comparison of Figs. 5 and 6 shows that the account for the change of the electronic structure with spin disordering is important for the understanding the SOC-caused effects in ferromagnetic systems disturbed by temperature or laser light.

To illustrate the influence of the modification of the electronic structure on the properties of the orbital moments we present in Fig. 2 the components of the atomic orbital moments calculated for noncollinear spin configuration with angle  $80^\circ$  between local atomic spin axes. The comparison of the curves shows that the spin noncollinearity leads to the narrowing of the peaks in agreement with the narrowing of the peaks of the DOS. There is also specific change in the form of the upper (spin-down) peak in the energy dependence of the  $x$  component of the orbital moment. For both Fe and Co a broader FM peak is transformed to a narrower peak followed by a wide shoulder. The crucial difference between Fe and Co is that in the case of Fe the Fermi level lies directly at the position of the peak leading to large  $x$  component of the orbital moment and increased MAE. On the other hand, in the case of Co, because of one extra 3d electron, the Fermi level is in the energy region of the shoulder. The comparison of the  $\theta_{\text{inter}}$

dependencies of the MAE and the anisotropy of the orbital moment (Fig. 4) show clear qualitative similarity of the pairs of dependencies for both Fe and Co films. The two curves for the same film, however, are not proportional to each other and there is no simple quantitative relation between them.

If we now plot MAE and  $\Delta m_o$  as a function of  $\theta_{\text{inter}}$  in the case of FePt (Fig. 4) we see that the behavior of  $\Delta m_o$  of Fe atoms does not follow Bruno's concept. For small  $\theta_{\text{inter}}$  we can establish correlation in the behavior of  $\Delta m_o$  of Pt atoms and MAE in the sense that they have opposite signs and both decrease with increase of  $\theta_{\text{inter}}$ . For larger angles the strong difference between curves becomes obvious. These results show nontrivial richness of the physics in binary systems combining a magnetic 3d element with a heavy 5d element. This richness cannot be captured on the basis of a simple qualitative consideration and needs detailed first-principles calculations.

We should remark that the present work is restricted to very simple noncollinear spin configurations that cannot reflect the whole complexity of the process of the spin disorder. A consequent investigation of the temperature effects should include the selection of the representative set of noncollinear configurations and the statistical-mechanics averaging with account for the energies of excited states. Such a study is not a part of the given paper.

#### IV. CONCLUSION

In conclusion, we performed calculation of the SOC-induced quantities of three itinerant-electron systems as a function of the angle between spin structure and crystallographic axes. Two results we consider as main findings of the work. First, we demonstrate by the example of FePt film that the presence of the competition of different SOC-caused processes leads to a remarkable property of the orthogonality of the inducing spin and induced orbital moments. Second, we demonstrate opposite trends in the variation of the MAE with increasing noncollinearity of atomic spins in Co and Fe films. We explain the diversity of behavior by the strong dependence of the electronic structure on spin disordering. This suggests a microscopic explanation to the long-standing challenging problem of the absence of a universal temperature behavior of the MAE in itinerant magnets.

<sup>1</sup>N. Nagaosa, J. Sinova, S. Onoda, A. H. MacDonald, and N. P. Ong, *Rev. Mod. Phys.* **82**, 1539 (2010).

<sup>2</sup>I. M. Miron, G. Gaudin, S. Auffret, B. Rodmacq, A. Schuhl, S. Pizzini, J. Vogel, and P. Gambardella, *Nat. Mater.* **9**, 230 (2010).

<sup>3</sup>M. Z. Hasan and C. L. Kane, *Rev. Mod. Phys.* **82**, 3045 (2010).

<sup>4</sup>G. H. O. Daalderop, P. J. Kelly, and M. F. H. Schuurmans, *Phys. Rev. B* **42**, 7270 (1990).

<sup>5</sup>J. Stöhr and H. König, *Phys. Rev. Lett.* **75**, 3748 (1995).

<sup>6</sup>C. Boeglin, E. Beaurepaire, V. Halte, V. Lopez-Flores, C. Stamm, N. Pontius, H. A. Dürr, and J.-Y. Bigot, *Nature (London)* **465**, 458 (2010).

<sup>7</sup>H. B. Callen and E. Callen, *J. Phys. Chem. Solids* **27**, 1271 (1966).

<sup>8</sup>M. Farle, W. Platow, E. Kosubek, and K. Baberschke, *Surf. Sci.* **439**, 146 (1999).

<sup>9</sup>K. Baberschke, *Lecture Notes in Physics*, Vol. 580 (Springer-Verlag, Berlin, 2001), p. 27.

<sup>10</sup>R. Skomski, A. Kashyap, A. Solanki, A. Enders, and D. J. Sellmyer, *J. Appl. Phys.* **107**, 09A735 (2010).

<sup>11</sup>P. Bruno, *Phys. Rev. B* **39**, 865 (1989).

<sup>12</sup>L. M. Sandratskii, *Adv. Phys.* **47**, 91 (1998).

<sup>13</sup>H. A. Dürr, G. Y. Guo, G. van der Laan, J. Lee, G. Lauhoff, and J. A. C. Bland, *Science* **277**, 213 (1997).

- <sup>14</sup>C. Nistor, T. Balashov, J. J. Kavich, A. Lodi Rizzini, B. Ballesteros, G. Gaudin, S. Auffret, B. Rodmacq, S. S. Dhesi, and P. Gambardella, *Phys. Rev. B* **84**, 054464 (2011).
- <sup>15</sup>C. Andersson, B. Sanyal, O. Eriksson, L. Nordström, O. Karis, D. Arvanitis, T. Konishi, E. Holub-Krappe, and J. H. Dunn, *Phys. Rev. Lett.* **99**, 177207 (2007).
- <sup>16</sup>Kh. Zakeri, Th. Kebe, J. Lindner, and M. Farle, *Phys. Rev. B* **73**, 052405 (2006).
- <sup>17</sup>C. Stamm, T. Kachel, N. Pontius, R. Mitzner, T. Quast, K. Holldack, S. Khan, C. Lupulescu, E. F. Aziz, M. Wietstruk, H. A. Dürr, and W. Eberhardt, *Nat. Mater.* **6**, 740 (2007).